

## Biosynthesis of LiFePO<sub>4</sub>/C Cathode Materials by a Sol-gel Route for Use in Lithium Ion Batteries

Linjing Chen<sup>1,2</sup>, Wangjun Feng<sup>1,2,\*</sup>, Wenxiao Su<sup>2</sup>, Miaomiao Li<sup>2</sup>, Changkun Song<sup>2</sup>

<sup>1</sup> State Key Laboratory of Advanced Processing and Recycling Nonferrous Metals, Lanzhou University of Technology, Lanzhou 730050, China

<sup>2</sup> School of Science, Lanzhou University of Technology, Lanzhou 730050, China

\* E-mail: [wjfeng@lut.cn](mailto:wjfeng@lut.cn)

Received: 22 November 2018 / Accepted: 4 January 2019 / Published: 7 February 2019

---

Based on the concepts of green science and environmental protection, LiFePO<sub>4</sub>/C is successfully encapsulated by the biomineralization of nontoxic and pollution-free yeast. A novel biosynthetic sol-gel method is applied to prepare LiFePO<sub>4</sub>/C, leading to an excellent electrochemical performance compared with that of conventional LiFePO<sub>4</sub>. Yeast acts as a biocarbon source in the preparation process. The effects of sintering temperature on the electrochemical properties of LiFePO<sub>4</sub>/C are studied. LiFePO<sub>4</sub>/C synthesized at 800°C exhibits the best rate capacity of 158.3 mAh/g at 0.1 C, and the discharge capacity remains at 94.3 mAh/g at 5 C after 100 cycles. These results prove that LiFePO<sub>4</sub>/C synthesized at 800°C has the promise to be a positive-anode active material with excellent properties.

---

**Keywords:** LiFePO<sub>4</sub>/C, biosynthesis, sol-gel method, electrochemical property, yeast.

### 1. INTRODUCTION

Energy forms the basis for human survival, which makes the emergence of new energy sources and the development of their related energy technologies very necessary [1–2]. The energy problem and the environmental problem are the two major challenges facing mankind. A number of studies, such as those on semiconductor-based photocatalysis and lithium-ion batteries (LIBs), have been performed to resolve the issues in energy storage [3]. In recent years, to solve the above problems, an increasing amount of research has been carried out on advanced materials for LIBs to meet the energy storage needs [4]. However, the energy and power densities must be further improved to expand the applications of LIBs in electric vehicles and large-scale energy storage. Among the many energy storage materials (LiCoO<sub>2</sub>, LiMn<sub>2</sub>O<sub>4</sub>, LiNiO<sub>2</sub> and LiFePO<sub>4</sub>), LiFePO<sub>4</sub> (LFP) has been widely studied

for its advantages, such as high specific capacity ( $170 \text{ mAh g}^{-1}$ ), good safety, superior capacity retention and environmental friendliness [5-7]. The major drawback of  $\text{LiFePO}_4$  originates from its low lithium-ion mobility and low electronic conductivity, which lead to a poor rate capacity and certain capacity loss [8]. A number of methods have been utilized to overcome these problems, such as metal doping, morphological changes and narrowing the particle sizes. It has been found that a carbon coating on the surface of  $\text{LiFePO}_4$  can not only improve the conductivity of the material [9-13] but also, due to its reducing property, prevent  $\text{Fe}^{2+}$  from being oxidized. CNTs coated onto LFP are considered to be an effective strategy to enhance the electronic conductivity and improve the electrochemical performance of LFP [14 15]. Nevertheless, most existing systems have low interfacial contact and inadequate surface coverage [16]. At present, numerous methods, such as solid-state [17], self-assembly of surface-modified  $\text{LiFePO}_4$  [18] and catalyst-assisted self-assembly [19], have been used to synthesize  $\text{LiFePO}_4$ -graphene composites. However, these methods are costly and complicated.

Biom mineralization refers to the process of generating inorganic minerals through the regulation of biological macromolecules by organisms [20-22]. Its advantage is that it can not only synthesize advanced functional materials but also control their crystal sizes. Yeast is harmless and easy to culture; it is found in air, soil, water and animals. It can be used as a carbon source. Biological mineralization has been widely studied. Cao et al. successfully prepared  $\text{LiFePO}_4/\text{C}$  by using yeast as a template and demonstrated that the yeast cells were able to control the formation of hollow microspheres and act as a biocarbon source [23]. Porous  $\text{TiO}_2$  has been prepared by Chang et al., in which yeast offer a meso/macro porous structure and are used as an electrode material [24]. Du et al. synthesized  $\text{Li}_3\text{V}_2(\text{PO}_4)_3$ -carbon microspheres, which showed a higher apparent diffusion coefficient for  $\text{Li}^+$  and a higher discharge capacity ( $126.7 \text{ mAh/g}$  at a rate of  $0.2 \text{ C}$ ) [25]. Inspired by the above research results, we use yeast as a carbon precursor to coat  $\text{LiFePO}_4$ , which not only controls the size of the particles but also regulates their morphology.

In this work,  $\text{LiFePO}_4$  (LFP) nanoparticles coated with carbon are synthesized by a biomimetic approach. The thin carbon layer can facilitate electrochemical reactivity and reversibility. LFP nanoparticles are noted as LFP/C and are abbreviated as LFP/C microspheres. The biggest advantage of this approach is the use of low-cost yeast as the template. We observe the structure and electrochemical properties of the material; at the same time, electrochemical impedance spectroscopy (EIS) is used to determine the diffusion coefficients.

## 2. EXPERIMENTS

### 2.1. Material preparation

Olivine-type  $\text{LiFePO}_4$  was prepared by a sol-gel method using  $\text{FeCl}_2 \cdot 4\text{H}_2\text{O}$ ,  $\text{LiOH} \cdot \text{H}_2\text{O}$  and  $\text{NH}_4\text{H}_2\text{PO}_4$  as the raw materials. The general experimental scheme can be described as follows. First, a quantitative amount of dry yeast was cultured at  $28^\circ\text{C}$  for 2 h in a glucose solution. The yeast was washed several times with distilled water. Second, a stoichiometric amount of  $\text{FeCl}_2 \cdot 4\text{H}_2\text{O}$  was

dissolved in 100 ml distilled water. The as-prepared yeast cells were added into the solution and stirred for 4 h. After that, solutions of  $\text{LiOH}\cdot\text{H}_2\text{O}$ ,  $\text{NH}_4\text{H}_2\text{PO}_4$  and  $\text{C}_6\text{H}_8\text{O}_7\cdot\text{H}_2\text{O}$  were mixed in stoichiometric amounts at room temperature.  $\text{C}_6\text{H}_8\text{O}_7\cdot\text{H}_2\text{O}$  was used as a chelating reagent. The obtained solution was transferred into a water bath kettle and heated to  $80^\circ\text{C}$  for several hours under vigorous stirring until the gel set. Subsequently, the gel was dried at  $140^\circ\text{C}$  for 12 h, and precursor LFP/C was obtained. Finally, the obtained powder was sintered in a muffle furnace at  $700^\circ\text{C}$ ,  $750^\circ\text{C}$ ,  $800^\circ\text{C}$  or  $850^\circ\text{C}$  for 6 h under nitrogen atmosphere, the samples of which were denoted as LFP/C-700, LFP/C-750, LFP/C-800 and LFP/C-850, respectively.

## 2.2. Materials Characterization

The phases of the as-prepared samples were identified using X-ray diffraction (XRD) utilizing  $\text{Cu K}\alpha$  radiation at 40 kV and 40 mA and collecting data from  $10^\circ$  to  $80^\circ$  ( $2\theta$  degree). The transmission electron microscope (TEM) images were collected with a JEM-2100F system at a voltage of 200 kV. The elemental composition of the LFP/C were determined by EDS equipped on an SEM.

## 2.3. Electrochemical analysis

Electrochemical characterization of the prepared composites was performed using CR-2025 coin-type cells. The cathode was fabricated by using LFP/C, polyvinylidene fluoride (PVDF) and Super P in a weight ratio of 80:10:10. The slurry was cast onto aluminum foil and then dried at  $120^\circ\text{C}$  under vacuum for 12 h. Cells were assembled in a glove box filled with argon and used Celgard 2400 as the separator. Li ribbon was used as the anode. The charging-discharging tests were conducted at room temperature with a Land CT2001A test system to investigate the rate performances and the cycle lifetimes (voltage range from 2 V to 4.2 V) at various discharging C-rates. Cyclic voltammetry (CV) measurements were obtained with a scanning rate of  $0.1 \text{ mVs}^{-1}$ . Electrochemical impedance spectroscopy (EIS) was carried out by an electrochemical workstation over a frequency range of 100 kHz-10 MHz.

# 3. RESULTS AND DISCUSSION

## 3.1. Crystalline structure analysis

To examine the crystal structures of the as-synthesized samples, the XRD patterns of all the LFP/C samples prepared at different sintering temperatures ( $700^\circ\text{C}$ ,  $750^\circ\text{C}$ ,  $800^\circ\text{C}$  and  $850^\circ\text{C}$ ) are shown in Fig. 1. The phases of all the samples confirm the orthorhombic olivine-type structure of  $\text{LiFePO}_4$  (JCPDS NO.83-2092) [26] without extra peaks, which indicates that the addition of yeast to the preparation of  $\text{LiFePO}_4$  did not affect its lattice structure. The reason for this may be that the high-

energy phosphate groups in yeast cells are negatively charged. Thus, these groups would bind preferentially with ferrous ions. Additionally, the high-energy phosphate groups are the most important contributor to the free energy barrier of iron phosphate biomineralization. From the analysis of the XRD patterns, no characteristic diffraction peaks for carbon are found, suggesting that the carbon in the material had an amorphous structure. The diffraction peaks of LFP/C-700, LFP/C-750 and LFP/C-850 become weaker and shift to some extent, which indicates that these materials are not sufficiently crystalline.

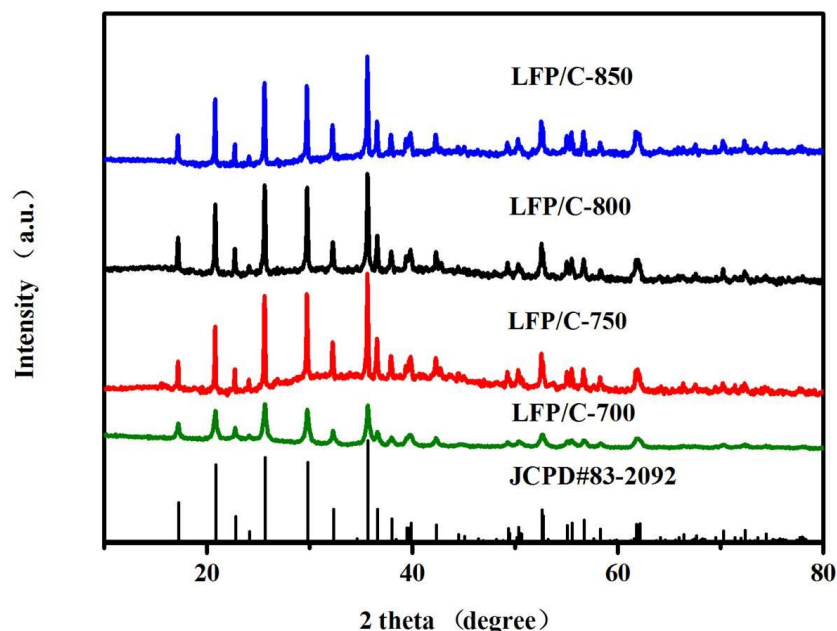


**Figure 1.** XRD patterns of the LFP/C samples formed at various temperatures

Crystal growth is effectively controlled by the carbon coating [27]. The particle size is important because it greatly affects the electrochemical properties and electrical conductivities of the electrode materials. The calculated structural parameters are listed in Table 1, according to the Scherrer formula and Bragg formula based on the full-width at half-maximum (FWHM). The crystal cell parameters for the lithium iron phosphates decrease slightly with increasing temperature due to the addition of the yeast cells.

**Table 1.** Unit cell parameters of all samples

Sample	a (Å)	b (Å)	c (Å)	Cell volume (Å <sup>3</sup> )
LFP/C-700	6.00973	10.33523	4.69293	291.48
LFP/C-750	6.00712	10.33082	4.69224	291.19

LFP/C-800	6.00704	10.32815	4.69137	291.06
LFP/C-850	6.00473	10.33131	4.68572	290.69

3.2 Morphological observation

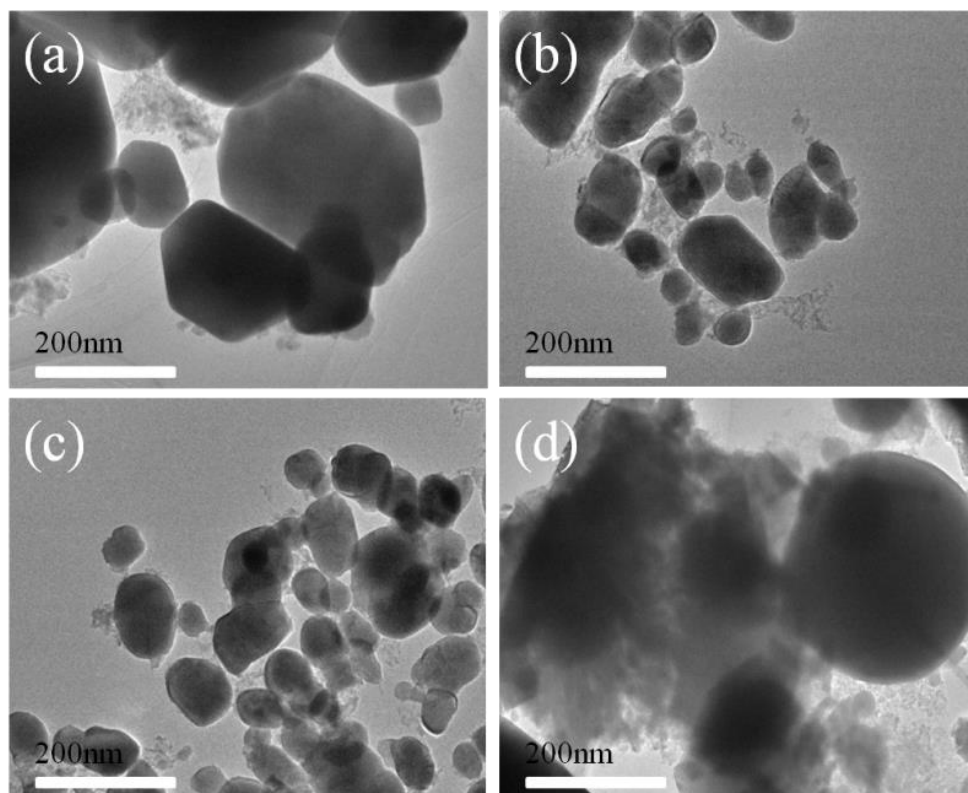


**Figure 2.** TEM images of the as-prepared LFP/C samples produced at different temperatures (a) LFP/C-700, (b)LFP/C-750, (c)LFP/C-800 and (d) LFP/C-850

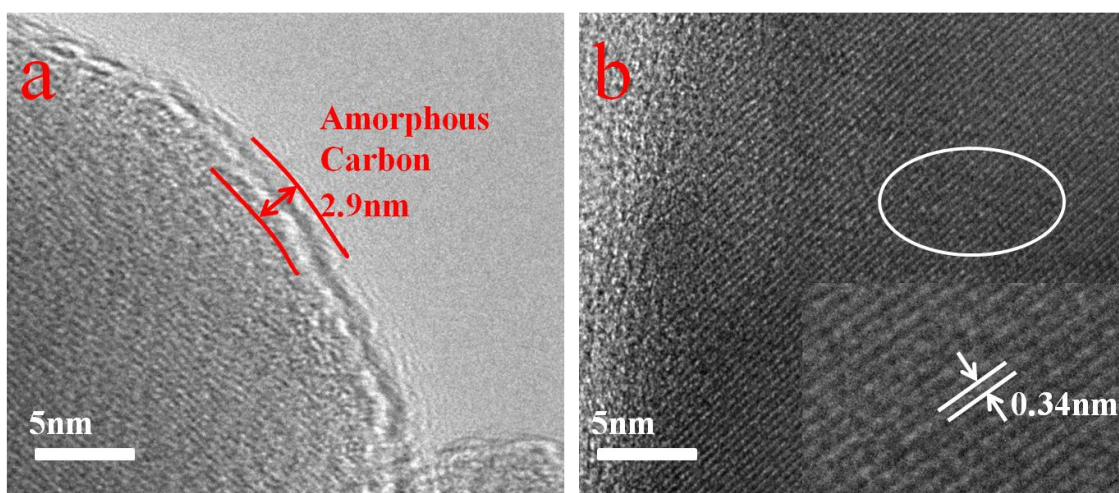


**Figure 3.** The magnified HRTEM images of LFP/C-800 (a,b)

The TEM images and HRTEM images of LFP/C-800 are shown in Fig. 2 and Fig. 3, which are conducive to identifying the effects of sintering temperature on particle size. In contrast, an important feature that can be seen is that the LFP/C-800 composite shows a smaller and more regular size than those of the other samples. The reason may be that with an increase in sintering temperature, the grains crystallize gradually and show a regular spherical shape. However, the morphology of LFP/C-850 is not clear under the same conditions. It could be that the temperature is too high for particles to agglomerate. It is obvious that the LiFePO<sub>4</sub> grains are uniformly covered by carbon. In the HRTEM image, the gray region and the dark region correspond to carbon and LiFePO<sub>4</sub>, respectively, implying that the outer layer of LiFePO<sub>4</sub> is surrounded by carbon. The thickness of the carbon layer is approximately 2.9 nm, indicating that yeast can be used as a carbon source in the process of preparing LFP. The carbon layer not only enhances the electronic conductivity but also prevents corrosion of the material [28]. Obviously, the particles are confined by the network structure of carbon. The same results were obtained in the XRD observations. Yeast is the cheapest source of carbon compared to those used in previously reported LFP cathode materials (Table 2.). Using yeast as a carbon source and a templating agent, we prepared a thinner carbon coating on a uniform positive electrode material that facilitates the insertion and extraction of lithium ions.

**Table 2.** Comparison with other currently reported carbon materials

Carbon source	Price	The thickness of the carbon layer	Reference
graphene	very expensive	5 nm	11
polyvinyl alcohol	expensive	4~5 nm	10
yeast	cheap	20.37 nm	23
yeast	cheap	2.9 nm	this work

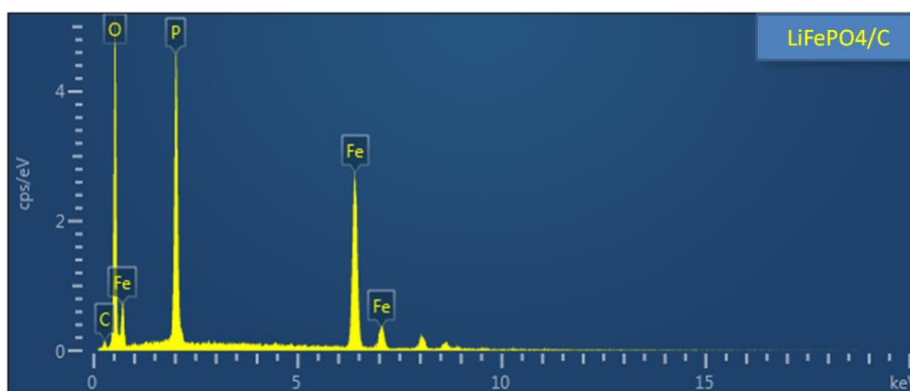


**Figure 4.** EDS spectrum for LFP/C-800

The EDS results reflect the amount of elements in the prepared materials [29]. The EDS spectrum of the  $\text{LiFePO}_4/\text{C}$  material synthesized at  $800^\circ\text{C}$  is shown in Fig. 4. The EDS spectrum and TEM images of the  $\text{LiFePO}_4/\text{C}$  composite prepared at  $800^\circ\text{C}$  confirm one another. EDS reveals that only C, O, Fe and P elements exist in the prepared material without the inclusion of impurity elements, which was also demonstrated by the XRD results. The contents of carbon in samples LFP/C-700, LFP/C-750, LFP/C-800 and LFP/C-850 are 5.24 wt%, 3.86 wt%, 3.21 wt% and 2.27 wt%, respectively. This indicates that the carbon content decreased with increasing sintering temperature, which is very important to the properties of  $\text{LiFePO}_4/\text{C}$ . The conductivity of the  $\text{LiFePO}_4/\text{C}$  material is related to the intrinsic conductivity of carbon.

### 3.3 Electrochemical performances

The electrochemical performances of the synthesized  $\text{LiFePO}_4/\text{C}$  materials were tested by galvanostatic charge/discharge measurements, which show the effects of sintering temperature on the electrochemical properties. The initial charge/discharge voltage profiles of the samples at 0.1 C are presented in Fig. 5. The cell performance depends greatly on the sintering temperature. The sample sintered at  $800^\circ\text{C}$  exhibits the best discharge capacity (158.3 mAh/g). The discharge capacities of LFP/C-700, LFP/C-750 and LFP/C-850 are approximately 117.1 mAh/g, 143.4 mAh/g and 132.6 mAh/g, respectively. The grain size and crystallinity of the material strongly influence the capacity. Compared with the capacity of other organic carbon sources, the  $\text{LiFePO}_4/\text{C}$  composite electrode materials prepared with yeast as the carbon source have a higher capacity [30-33]. D. Morgan and co-workers found that lithium ions diffuse through the one-dimensional channels in the olivine crystal structure [34]. The reason for this improved capacity may be that good one-dimensional channels, small particle sizes and an effective carbon coating layer are formed during the preparation of  $\text{LiFePO}_4/\text{C}$  when yeast is used as the carbon source and sintered at  $800^\circ\text{C}$ .

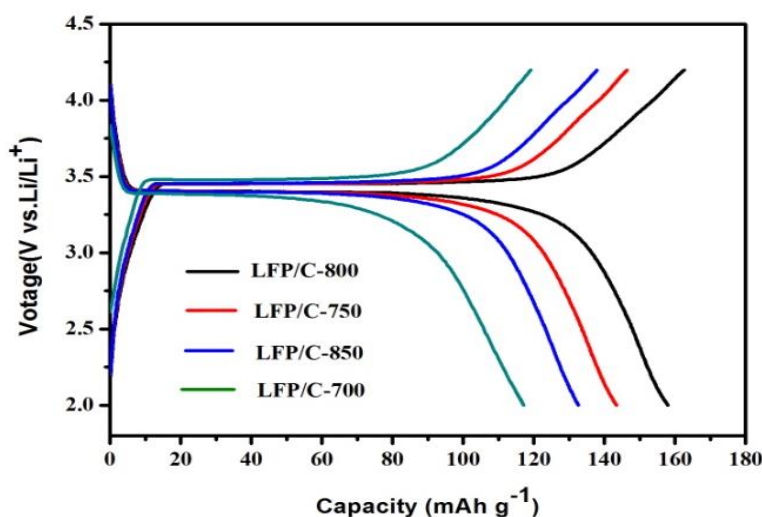


**Figure 5.** The first charge/discharge curves at 0.1 C of LFP/C-700, LFP/C-750, LFP/C-800 and LFP/C-850

The cycling performance of the LFP/C-800 electrode measured at room temperature over more than 100 cycles at rates of 0.2 C, 0.5 C and 5 C are shown in Fig. 6a. The LFP/C-800 electrode exhibits excellent charge-discharge cycling stability without significant decline of the capacity after 100 cycles. This may be because the smaller particle sizes facilitate the diffusion of the lithium ions. The LFP/C-800 also delivered approximately 96.6% of the initial capacity at 5 C. The diagram provides evidence of the excellent performance and cyclic stability of this sample, although there is a capacity loss. The reason may be that the LFP active material is in contact with the electrolyte for an extended time, which produces side reactions and leads to the loss of active material. For a more detailed understanding of the effects of the sintering temperature on the electrochemical properties of the samples that were sintered at 700°C, 750°C, 800°C and 850°C, the discharge capacities at various scanning rates were measured (shown in Fig. 6b). It can be found that LFP/C-800 exhibits the best specific capacity, which may be attributed to its perfect crystallinity.

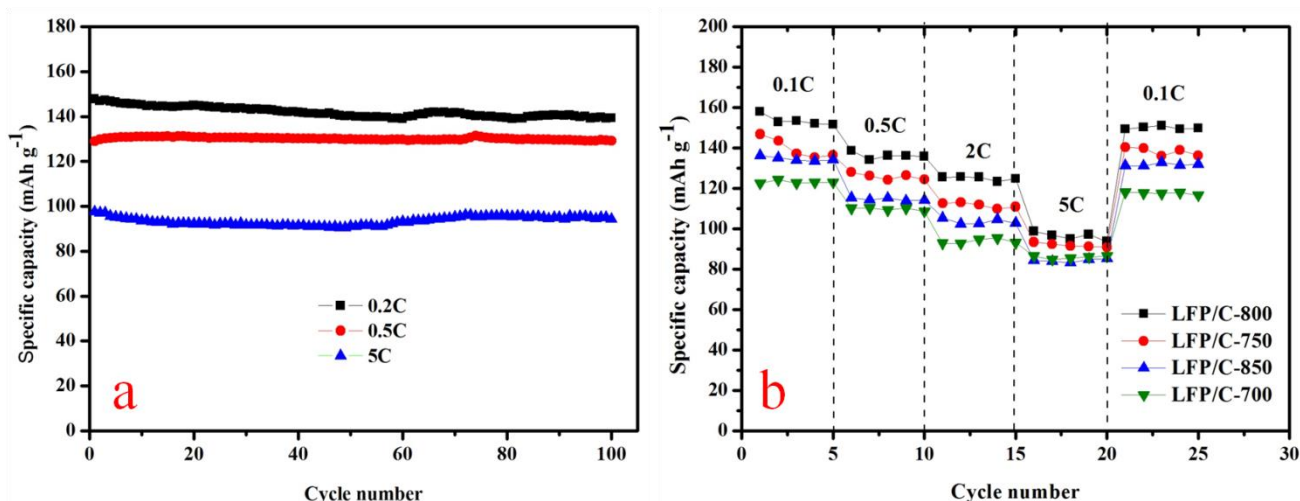


**Figure 6.** (a) Cycling performance of the LFP/C-800 at 0.2C, 0.5C and 5C (b) Cyclability of the LiFePO<sub>4</sub>/C-700, LiFePO<sub>4</sub>/C-750, LiFePO<sub>4</sub>/C-800 and LiFePO<sub>4</sub>/C-850 at various c-rates.

The results of the CV measurements are shown in Fig. 7a, which was carried out from 2.5-4.2 V at a scan rate of 0.1 mV/s. The LFP/C-800 sample shows a pair of sharp redox peaks, indicating that insertion/extraction processes occur at these potentials. Lithium ions are extracted from the LFP/C-800 anode material during redox scanning, corresponding to the oxidation peak and the reduction peak. The potential interval between the oxidation and reduction peaks of LFP/C-800 is 0.36 V, indicating a lower degree of polarization. Between the second cycle scan and that of the third cycle, the CV curves of the sample are very reproducible, demonstrating that LFP/C-800 has good cyclic stability. This is consistent with the cycling performance, which is shown in Fig. 6a. Therefore, we can consider the material to have good dynamic characteristics. Fig. 7b shows the EIS curves, which are made up of a semicircle in the high-medium frequency region and a slanted line in the low frequency region. The charge-transfer resistance relates to the semicircle in the high range [35]. The slope of the line refers to the diffusion resistance. The resistance of the LFP/C-800 electrode shows a smaller semicircle than that of the other samples, which indicates that this material exhibits favorable reaction kinetics during the electrochemical reaction compared to the samples sintered at 700°C, 750°C, 800°C and 850°C for 6

h. The LFP/C-800 material exhibits the minimum charge transfer resistance compared with that of LFP/C-700, LFP/C-750 and LFP/C-850 due to the increase in the electronic conductivity induced by the carbon coating. The results of EIS prove that using yeast as a carbon source for coating LiFePO<sub>4</sub> can significantly enhance the electrochemical performance of LFP/C-800 by improving the electronic conductivity and lithium ion diffusivity.

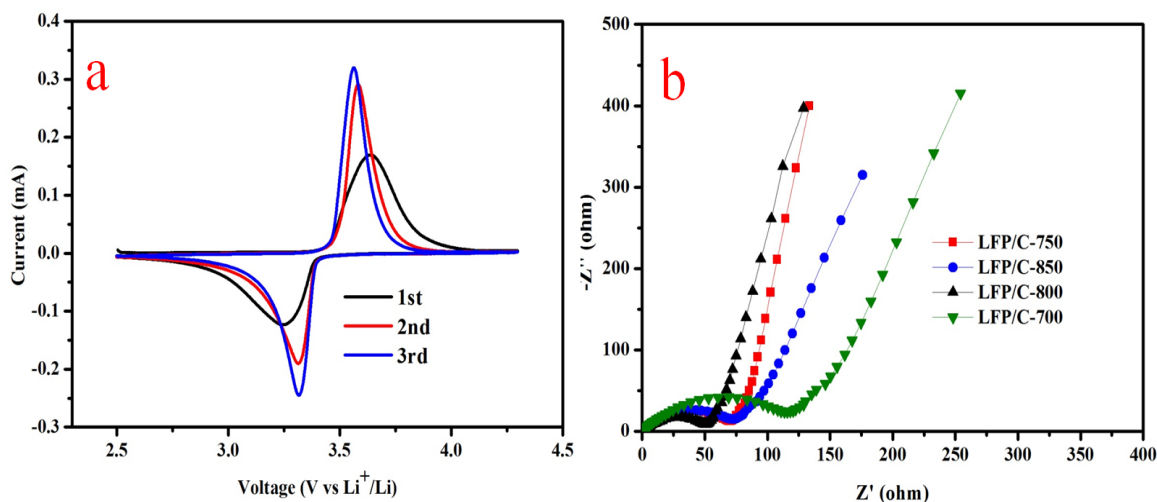


**Figure 7.** (a) Cyclic voltammetry profiles of LFP/C-800 and (b) EIS results of the samples of LFP/C-700, LFP/C-750, LFP/C-800 and LFP/C-850

#### 4. CONCLUSIONS

In summary, we have successfully prepared high performance LiFePO<sub>4</sub>/C materials via a controllable biosynthetic method at a moderate temperature (800°C). Instant yeast cells are used as a carbon source, whose coating onto the surface of the material has a significant effect on the impedance. During the sintering process, the surface carbon can control the size of the LiFePO<sub>4</sub> particles. Carbon can also enhance the electronic conductivity. The discharge specific capacity (158.3 mAh/g at 0.1 C) is much improved compared to that of standard LiFePO<sub>4</sub> because of the small size and good electronic conductivity of this material. The conductive network formed by the yeast provides short diffusion pathways for electrons and lithium ions. As the temperature further increased, the specific discharge capacity decreases, possibly because the conductive network was destroyed. However, through biomimetic material design and controlled preparation, this LiFePO<sub>4</sub> cathode material is promising for use in high-power applications.

#### ACKNOWLEDGMENTS

This work was financially supported by the National Natural Science Foundation of China (Grant No.11264023).

## References

- 1 S. W. Lee, N. Yabuuchi, B. M. Gallant, S. Chen, B.-S. Kim, P. T. Hammond and Y. Shao-Horn, *Nat. Nanotechnol.*, 5(2010) 531.
- 2 J. B. Goodenough, *Energy Env. Sci.*, 7(2014) 14.
- 3 Y. Yan, H. Yang, X. Zhao, R. Li and X. Wang, *Mater. Res. Bull.*, 105(2018) 286.
- 4 W. Su, W. Feng, Y. Cao, L. Chen, M. Li and C. Song, *Int. J. Electrochem. Sci.*, 13(2018)6005.
- 5 C. Gong, Z. Xue, S. Wen, Y. Ye and X. Xie, *J. Power Sources*, 318(2016) 93.
- 6 W. Lin Wang, V. Hiep Nguyen, E. Mei Jin and H.-B. Gu, *Mater. Express*, 3(2013)273.
- 7 T. Vranken, W. Van Gompel, J. D'Haen, M. K. Van Bael and A. Hardy, *J. Sol-Gel Sci. Technol.*, 84(2017)198.
- 8 L.-L. Zhang, G. Liang, A. Ignatov, M. C. Croft, X.-Q. Xiong, I.-M. Hung, Y.-H. Huang, X.-L. Hu, W.-X. Zhang and Y.-L. Peng, *J. Phys. Chem. C*, 115(2011)13520.
- 9 D. Zhou, X. Qiu, F. Liang, S. Cao, Y. Yao, X. Huang, W. Ma, B. Yang and Y. Dai, *Ceram. Int.*, 43(2017) 13254.
- 10 Y. Wang, Z. Liu and S. Zhou, *Electrochimica Acta*, 58(2011)359.
- 11 C. Su, X. Bu, L. Xu, J. Liu and C. Zhang, *Electrochimica Acta*, 64(2012)190.
- 12 G. Huang, W. Li, H. Sun, J. Wang, J. Zhang, H. Jiang and F. Zhai, *Electrochimica Acta*, 97(2013) 92.
- 13 Y. Tang, F. Huang, H. Bi, Z. Liu and D. Wan, *J. Power Sources*, 203(2012)130.
- 14 X.-Y. Liu, H.-J. Peng, Q. Zhang, J.-Q. Huang, X.-F. Liu, L. Wang, X. He, W. Zhu and F. Wei, *ACS Sustain. Chem. Eng.*, 2(2013)200.
- 15 S. Xin, Y.-G. Guo and L.-J. Wan, *Acc. Chem. Res.*, 45(2012)1759.
- 16 L. Tan, Q. Tang, X. Chen, A. Hu, W. Deng, Y. Yang and L. Xu, *Electrochimica Acta*, 137(2014)344.
- 17 J. Yang, J. Wang, D. Wang, X. Li, D. Geng, G. Liang, M. Gauthier, R. Li and X. Sun, *J. Power Sources*, 208(2012)340.
- 18 W.-B. Luo, S.-L. Chou, Y.-C. Zhai and H.-K. Liu, *J. Mater. Chem. A*, 2(2014) 4927.
- 19 W. Kim, W. Ryu, D. Han, S. Lim, J. Eom and H. Kwon, *ACS Appl. Mater. Interfaces*, 6(2014)4731.
- 20 C. Gröger, K. Lutz and E. Brunner, *Cell Biochem. Biophys.*, 50(2007)23.
- 21 S. B. Mukkamala, C. E. Anson and A. K. Powell, *Journal of Inorganic Biochemistry*, 100(2006) 1128
- 22 B. M. Borah, B. J. Bhuyan and G. Das, *J. Chem. Sci.*, 118(2006)519.
- 23 Y. Cao, W. Feng and W. Su, *Int. J. Electrochem. Sci.*, 12 (2017) 9084.
- 24 Y.-C. Chang, C.-Y. Lee and H.-T. Chiu, *ACS Appl. Mater. Interfaces*, 6(2013)31.
- 25 X. Du, W. He, X. Zhang, Y. Yue, H. Liu, X. Zhang, D. Min, X. Ge and Y. Du, *J. Mater. Chem.*, 22(2012)5960.
- 26 J. Song, B. Sun, H. Liu, Z. Ma, Z. Chen, G. Shao and G. Wang, *ACS Appl. Mater. Interfaces*, 8(2016)15225.
- 27 W. Li, J. Hwang, W. Chang, H. Setiadi, K. Y. Chung and J. Kim, *J. Supercrit. Fluids*, 116(2016)164.
- 28 R. Wu, G. Xia, S. Shen, F. Zhu, F. Jiang and J. Zhang, *RSC Adv.*, 4(2014)21325.
- 29 N. Bai, K. Xiang, W. Zhou, H. Lu, X. Zhao and H. Chen, *Electrochimica Acta*, 191(2016)23.
- 30 P. M. Pratheeksha, E. H. Mohan, B. V. Sarada, M. Ramakrishna, K. Hembram, P. V. V. Srinivas, P. J. Daniel, T. N. Rao and S. Anandan, *Phys. Chem. Chem. Phys.*, 19(2017)175.
- 31 S. Qiu, X. Zhang, Y. Li, T. Sun, C. Wang and C. Qin, *J. Mater. Sci. Mater. Electron.*, 27(2016)7255.
- 32 R. Scipioni, P. S. Jørgensen, D.-T. Ngo, S. B. Simonsen, Z. Liu, K. J. Yakal-Kremiski, H. Wang, J. Hjelm, P. Norby, S. A. Barnett and S. H. Jensen, *J. Power Sources*, 307(2016)259.

- 33 O. Y. Posudievsky, O. A. Kozarenko, V. S. Dyadyun, V. G. Koshechko and V. D. Pokhodenko, *J. Solid State Electrochem.*, 19(2015)2733.
- 34 D. Morgan, A. Van der Ven and G. Ceder, *Electrochem. Solid-State Lett.*, 7(2004)A30.
- 35 R. Chen, Y. Wu and X. Y. Kong, *J. Power Sources*, 258(2014)246.

© 2019 The Authors. Published by ESG ([www.electrochemsci.org](http://www.electrochemsci.org)). This article is an open access article distributed under the terms and conditions of the Creative Commons Attribution license (<http://creativecommons.org/licenses/by/4.0/>).